LETTER

doi:10.1038/nature11200

Late Miocene decoupling of oceanic warmth and atmospheric carbon dioxide forcing

Jonathan P. LaRiviere[1], A. Christina Ravelo[1], Allison Crimmins[1]†, Petra S. Dekens[1]†, Heather L. Ford[1], Mitch Lyle[2] & Michael W. Wara[1]†

Deep-time palaeoclimate studies are vitally important for developing a complete understanding of climate responses to changes in the atmospheric carbon dioxide concentration (that is, the atmospheric partial pressure of CO_2, p_{CO_2})[1]. Although past studies have explored these responses during portions of the Cenozoic era (the most recent 65.5 million years (Myr) of Earth history), comparatively little is known about the climate of the late Miocene (~12–5 Myr ago), an interval with p_{CO_2} values of only 200–350 parts per million by volume but nearly ice-free conditions in the Northern Hemisphere[2,3] and warmer-than-modern temperatures on the continents[4]. Here we present quantitative geochemical sea surface temperature estimates from the Miocene mid-latitude North Pacific Ocean, and show that oceanic warmth persisted throughout the interval of low p_{CO_2} ~12–5 Myr ago. We also present new stable isotope measurements from the western equatorial Pacific that, in conjunction with previously published data[5–10], reveal a long-term trend of thermocline shoaling in the equatorial Pacific since ~13 Myr ago. We propose that a relatively deep global thermocline, reductions in low-latitude gradients in sea surface temperature, and cloud and water vapour feedbacks may help to explain the warmth of the late Miocene. Additional shoaling of the thermocline after 5 Myr ago probably explains the stronger coupling between p_{CO_2}, sea surface temperatures and climate that is characteristic of the more recent Pliocene and Pleistocene epochs[11,12].

High-latitude climate reconstructions from the oxygen isotopic composition ($\delta^{18}O$) of benthic foraminifera[3] reveal a long-term cooling trend over the past ~50 Myr that occurred in conjunction with decreasing p_{CO_2} (ref. 2). However, although CO_2 levels were near pre-industrial values (280 p.p.m.v.) during the late Miocene (even the highest end of both the alkenone and leaf stomata estimates of CO_2 indicate that late Miocene CO_2 levels were less than the modern values of ~390 p.p.m.v.), high-latitude climate was too warm to support the growth of large Northern Hemisphere ice sheets[2,3] (Fig. 1a, f and Supplementary Information).

Climate modellers have tested whether external boundary conditions, such as the reduced topography of mountainous regions during the late Miocene[13], could have lowered the p_{CO_2} threshold for glaciation[14–16]; however, these tests focused on regional ice sheet growth rather than global temperatures and have not accounted for climate conditions outside the high latitudes. Palaeoclimate estimates from vegetation reconstructions suggest that warmer-than-modern conditions existed not just in the high latitudes but were globally widespread ~12–7 Myr ago[4] (Supplementary Information). Vegetation probably acted as a strong warming feedback in the late Miocene[17]; however, the boundary conditions that underlie such a vegetation distribution are not well constrained. Ocean circulation would have been integral to the global climate system of the late Miocene, but very little quantitative data exist to constrain surface circulation. For this reason, we reconstructed changes in sea surface temperature (SST) in the mid-latitude North Pacific Ocean and monitored the depth of the western tropical Pacific thermocline (the boundary between the warm surface ocean layer and the subsurface cold deep ocean) for the past ~13 Myr.

The SST estimates are derived from sediments collected at three Ocean Drilling Program (ODP) sites: Site 1010 (30° N, 118° W) in the subtropical east Pacific; Site 1021(39° N, 128° W) in the northeast Pacific at the seaward side of the northern edge of the California Current; and Site 1208 (36° N, 158° E) in the northwest Pacific at the transition zone between the subtropical and subarctic gyres (Fig. 2). SST estimates are based on the alkenone unsaturation proxy ($U^{k'}_{37}$) using the calibration of ref. 18. The 1010 and 1021 SST reconstructions are continuous since ~13 Myr before present. The SST reconstruction from Site 1208 is continuous since ~10 Myr before present.

The warmest SSTs occurred at the beginning of the late Miocene with subsequent cooling over the length of all three records. At subtropical east Pacific Site 1010, SSTs cooled by 5 °C between 9 and 5.8 Myr ago, and cooled an additional ~8 °C from the early Pliocene warm period, about 3.7 Myr ago, into the recent Pleistocene ice ages (Fig. 1e). A similar pattern of SST cooling was observed at northeast Pacific Site 1021; SSTs cooled by ~5 °C by 5.8 Myr ago and, after a ~3 °C increase from ~5.8 to 4.5 Myr ago, subsequently cooled an additional ~8.5 °C into the ice ages (Fig. 1e). At the northwest Pacific Site 1208, SSTs decreased by ~3 °C by 5.8 Myr ago, and continued to cool by an additional ~4 °C from 2.7 Myr ago and into the ice ages (Fig. 1d). Overall, when compared to SST estimates from the western Pacific warm pool[5], our new records of warm subtropical SSTs reveal that late Miocene meridional SST gradients were reduced relative to those of the Pliocene. Site movement by plate tectonics from one ocean temperature regime to another can explain no more than ~2 °C of the SST trend since 13 Myr ago (Supplementary Information).

Our SST records provide, despite some regional variability, the first documentation that late Miocene SSTs across a broad swathe of the North Pacific were significantly warmer than present (by 5–8 °C), and that there was nearly unidirectional cooling over the past 13 Myr. Furthermore, our records are consistent with other palaeodata[4,13,19], including bottom-water temperature estimates[19] (Fig. 1b), which indicate that the climate was warmer during the late Miocene than during the early Pliocene warm period. Thus, the preponderance of data, including our new records, indicates that global temperatures of the late Miocene, with relatively low p_{CO_2} of <350 p.p.m.v., exceeded that of the early Pliocene warm period, with relatively high p_{CO_2} of >350 p.p.m.v. (Fig. 1f). This decoupling between temperature and atmospheric p_{CO_2} trends requires an explanation. One possibility is that changes in boundary conditions (for example, continental topography, ocean basin shape) played a major role in determining the sensitivity of Earth's climate to CO_2 forcing.

During the late Miocene, the Central American Seaway (CAS) was open, the Indonesian Seaway was wider than at present, and the Bering

[1]Ocean Sciences Department, University of California, Santa Cruz, California 95064, USA. [2]Department of Oceanography, Texas A&M University, College Station, Texas 77843, USA. †Present addresses: US Environmental Protection Agency, Climate Change Division, Washington DC 20460, USA (A.C.); Department of Geosciences, San Francisco State University, San Francisco, California 94132, USA (P.S.D.); Freeman Spogli Institute for International Studies, Stanford Law School, Stanford, California 94305, USA (M.W.W.).

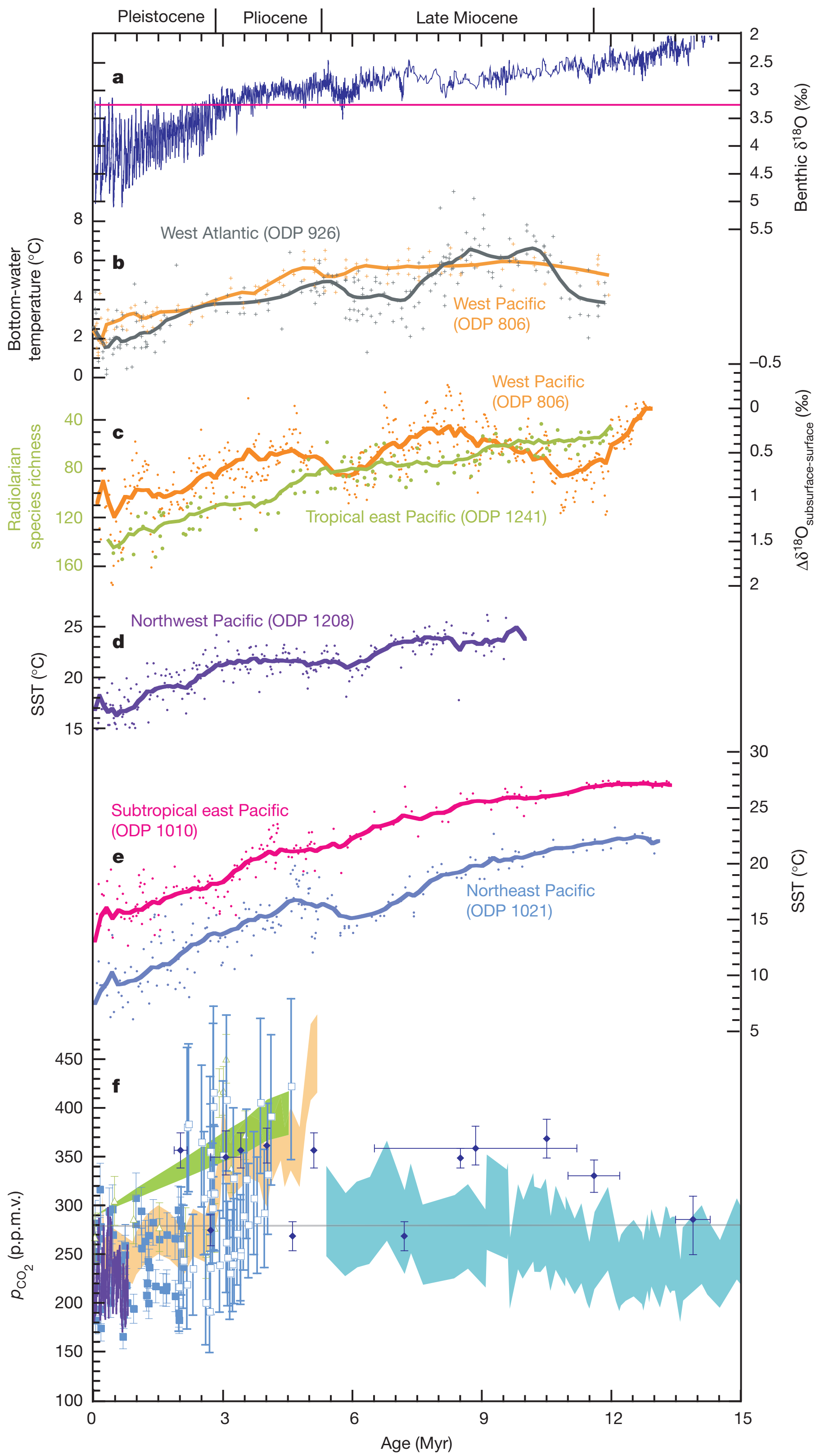

Figure 1 | Late Neogene oceanic conditions and atmospheric p_{CO_2}. **a**, Benthic foraminifera δ^{18}O record of high-latitude climate change[3,30]. Pink line denotes modern δ^{18}O. **b**, Mg/Ca-derived bottom-water temperatures from ODP Sites 806 and 926 (ref. 19). **c**, Oxygen isotopic difference between thermocline and surface foraminifera from Site 806 (orange curve, right-hand vertical axis) is inversely related to thermocline depth[5–7]. Radiolarian species richness from Site 1241[10] (green curve, left-hand vertical axis) is a reflection of thermocline depth. **d**, Alkenone SST estimates from Site 1208. **e**, Alkenone SST estimates from Sites 1021 and 1010. **f**, Estimates of atmospheric p_{CO_2} from ice cores (purple line), boron isotopes (open squares, filled squares and triangles), alkenones (green[11], gold and blue shading), and leaf stomata (diamonds). Grey line marks pre-industrial p_{CO_2} concentrations (280 p.p.m.v.). Vertical error bars represent reported uncertainty in boron isotope and leaf stomata p_{CO_2} estimates. Reported age uncertainties for leaf stomata estimates are denoted with horizontal bars. Green, gold and blue shading indicates the range between published maximum and minimum alkenone p_{CO_2} estimates. See Supplementary Information for p_{CO_2} data sources. Heavy lines in **b**–**e** represent Stineman smoothing curves applied in KaleidaGraph software (v4.1.3; http://www.synergy.com/).

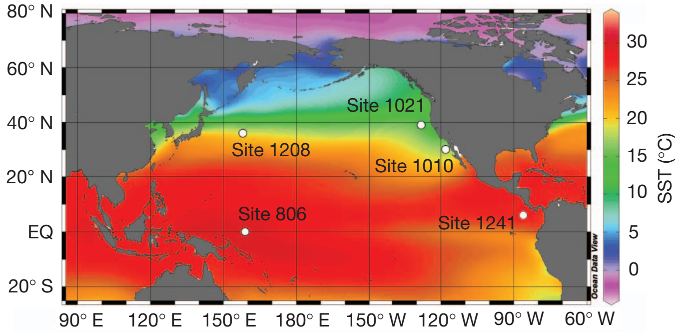

Figure 2 | Sites used in this study. ODP Sites 1208 (36° N, 158° E), 1021 (39° N, 128° W), 1010 (30° N, 118° W), 806 (0° N, 159° E) and 1241 (6° N, 86° W) overlaid on a map of mean annual SSTs[31]. EQ, Equator.

Strait was closed[13]; however, by the end of the early Pliocene the CAS was closed, the geography of the Indonesian Seaway was more similar to its modern configuration, and the Bering Strait was open[13]. Although none of the existing modelling sensitivity studies indicate that these tectonic changes could directly explain the warm, mid-latitude North Pacific temperatures observed in our reconstructions[20,21], modelling of the early Pliocene climate (5–3 Myr ago) does suggest that the CAS may have played a role in determining the depth of the thermocline. Results from general circulation models indicate that when the CAS was open, the modelled tropical thermocline was deeper[22,23], consistent with observations of the tropical Pacific thermocline[5–10,22]. Such a change in thermocline depth is important, because the ventilated thermocline maintains the balance between high-latitude oceanic heat loss and low-latitude heat gain[24]; a change in thermocline depth implies changes in surface ocean conditions that determine cloud, atmospheric water vapour and SST distributions[25]. Thus, changes in thermocline depth may be driven by internal dynamics or by changes in external boundary conditions, such as oceanic gateways, and could help to explain the climate of the late Miocene.

To assess changes in the shallow, wind-driven circulation of the ventilated thermocline, we monitored relative changes in thermocline depth at west Pacific ODP Site 806 (0° N, 159° E) (Fig. 2) using the $\delta^{18}O$ values of shells from surface-dwelling and subsurface-dwelling planktonic foraminifera. We made new stable isotopic measurements of *Globorotalia tumida* for the interval of ~4.8–0 Myr ago, which, in conjunction with previously published data[5–7] on this and other species, provides records of the $\delta^{18}O$ of *Globigerinoides sacculifer*, a surface dweller, and of *G. tumida*/*Globorotalia menardii*/*Globorotalia fohsi*, subsurface dwellers, for the past ~13 Myr. The difference between these species, $\Delta\delta^{18}O_{subsurface\text{-}surface}$, reflects thermocline depth[5–7], with low values indicating a thick mixed layer and deep thermocline, and high values indicating a thinner mixed layer and shallower thermocline. Whereas the previously published data showed two pronounced intervals of a relatively thin mixed layer ~13–11 and ~7–5.8 Myr ago, the additional isotopic data in our study reveal a long-term trend in $\Delta\delta^{18}O_{subsurface\text{-}surface}$ and indicate that the western equatorial Pacific thermocline has gradually shoaled since ~13 Myr ago (Supplementary Information). Evidence for thermocline changes in the eastern tropical Pacific comes from radiolarian species richness (ODP 1241; 6° N, 86° W), which shows a monotonic increase since ~12 Myr ago[10], and is consistent with a long-term increase in the number of ecological niches available as the thermocline became shallower (Fig. 1c). In addition, the authors of ref. 10 interpreted the radiolarian assemblage changes since ~4.2 Myr ago to indicate the shoaling of the eastern tropical Pacific thermocline from a relatively deep configuration that existed for the majority, if not all, of the late Miocene. Furthermore, foraminifera faunal reconstructions throughout the tropical Pacific show that the thermocline has generally shoaled from a relatively deep position in the middle Miocene to a shallower depth by the end of the late Miocene[8,9].

Overall, our data indicate that the oceanic state of the late Miocene was similar to that of the early Pliocene warm period, though more extreme (with warmer SSTs, smaller SST gradients and a deeper thermocline). Modelling of the early Pliocene conditions demonstrates that a tight coupling between the deep thermocline, expanded tropical warmth, and the reduction in meridional and zonal SST gradients resulted in mean global temperatures 3–4 °C warmer than today and the suppression of Northern Hemisphere glaciation[26]. The models, which are constrained by Pliocene proxy data, show that the expanded tropical warmth results in enhanced subtropical evaporation, greenhouse warming from water vapour, and warming from an increase in subtropical high 'greenhouse clouds'. These processes form a feedback loop that further facilitates maintenance of a deep thermocline and a warm climate with expanded tropical warmth[27]. Applying this idea to the Miocene provides a framework to understand our new SST and thermocline observations, all of which are consistent with warmer-than-modern global temperatures, as is the case in the early Pliocene. Furthermore, when applied to the Miocene, the Pliocene body of work suggests that, in the absence of large changes in p_{CO_2}, a tectonically driven change in upper ocean structure and tropical warm pool expanse could have, by itself, affected global temperatures through changes in atmospheric water vapour (a greenhouse gas) concentrations and in planetary albedo (through cloud type and distribution).

Changes in thermocline depth could explain the differences between late Miocene and Pliocene climate responses to atmospheric p_{CO_2} forcing. The shoaling of the thermocline has been directly linked to intensification of tropical SST gradients[22,28] and the strength of Walker and Hadley atmospheric circulation. However, when the thermocline is sufficiently deep (as it was in the tropical Pacific during the late Miocene), its movement is not coupled with SSTs. An increase in coupling appears to occur when the thermocline is shallow enough to pass some threshold depth. This threshold can explain why the thermocline depth variation in the western equatorial Pacific—a region where the thermocline is currently deeper than the surface Ekman layer of wind-driven mixing—did not appear to be coupled to SSTs until the thermocline in the eastern tropical Pacific shoaled adequately; such shoaling happened in the early Pliocene or, at the earliest, during the conclusion of the late Miocene. Once the thermocline became sufficiently shallow to affect SSTs, the climate system seems to have become sensitive to climate perturbations that had previously been inconsequential, including those driven by changes in p_{CO_2}. For example, with a shallow thermocline any small change (for example, in winds or in upwelling strength) that affected the low-latitude SSTs would be accompanied by strong positive feedbacks; changes in surface pressure gradients could reinforce initial changes in winds and in atmospheric water vapour and cloud formation[26] that amplify global temperature change. A shallower thermocline and accompanying enhanced climate sensitivity could explain why the Northern Hemisphere ice ages began in the Pliocene, rather than in the Miocene at comparable p_{CO_2} levels, and why a close coupling between glacial–interglacial climate cycles and p_{CO_2} developed after ~2.7 Myr ago[29].

Differences in the oceanic gateway boundary conditions of the late Miocene and Pliocene may have been the ultimate cause of the increase in climate sensitivity to p_{CO_2} forcing; the ocean basin configuration of the Pliocene, rather than the configuration that existed for the majority of the late Miocene, enabled the thermocline to shoal past a depth that was critical for coupling the thermocline and SSTs. However, although the closing of the CAS is the best candidate for forcing major upper-ocean structure changes in the earliest Pliocene, much work is needed to verify this idea and to test the effects of other ocean gateways on thermocline depth. Future work should aim to increase the geographic coverage of the surface and subsurface oceanographic reconstructions with an emphasis on ocean gateway regions (for example, the CAS, Indonesian Seaway and Bering Strait). Such evidence would help to constrain the timing and the nature of ocean circulation change, and therefore climate change, associated with tectonic events in the late Miocene and early Pliocene.

METHODS SUMMARY

Lipids were extracted from 0.5–5 g of crushed sediment with either a 3:1 dichloromethane:methanol mix or pure dichloromethane using a Dionex ASE200 accelerated solvent extractor. The total lipid extract was evaporated to dryness under N_2 and redissolved in 100–200 μl of toluene with hexatriacontane and heptatriacontane internal standards. Separation of organic compounds was carried out on an HP6890 gas chromatograph equipped with a flame ionization detector. Long-term reproducibility of liquid standard replicates included in each gas chromatography run was within ±0.007 $U^{k'}_{37}$ units, which is equivalent to ±0.2 °C (s.d., $n = 139$). We monitored the long-term precision of the entire method by processing a sediment standard with each batch of samples. Reproducibility for the sediment standards used for the 1208, 1021 and 1010 sites was ±0.016 (s.d., $n = 25$), ±0.013 (s.d., $n = 27$) and ±0.015 (s.d., $n = 9$) $U^{k'}_{37}$ units, respectively. The standard error of the estimate for the global SST calibration of ref. 18 is ±1.5 °C.

Fossil shells of *G. tumida* were analysed for oxygen isotopic composition ($\delta^{18}O$) using a Fisons Prism III dual inlet isotope ratio mass spectrometer. The precision of NBS-19 (NIST-8544) and of an in-house Carrera Marble standard was better than 0.08‰ for $\delta^{18}O$. Measurements of $\delta^{18}O$ are reported relative to Vienna-Pee Dee Belemnite (V-PDB).

Received 15 November 2011; accepted 2 May 2012.

1. Hansen, J. *et al.* Target atmospheric CO_2: where should humanity aim? *Open Atmos. Sci. J.* **2,** 217–231 (2008).
2. Ruddiman, W. F. A paleoclimatic enigma? *Science* **328,** 838–839 (2010).
3. Zachos, J., Pagani, M., Sloan, L., Thomas, E. & Billups, K. Trends, rhythms, and aberrations in global climate 65 Ma to present. *Science* **292,** 686–693 (2001).
4. Pound, M. J. *et al.* A Tortonian (Late Miocene, 11.61–7.25 Ma) global vegetation reconstruction. *Palaeogeogr. Palaeoclimatol. Palaeoecol.* **300,** 29–45 (2011).
5. Nathan, S. A. & Leckie, R. M. Early history of the Western Pacific Warm Pool during the middle to late Miocene (~13.2–5.8 Ma): role of sea-level change and implications for equatorial circulation. *Palaeogeogr. Palaeoclimatol. Palaeoecol.* **274,** 140–159 (2009).
6. Wara, M. W., Ravelo, A. C. & Delaney, M. L. Permanent El Niño-like conditions during the Pliocene warm period. *Science* **309,** 758–761 (2005).
7. Chaisson, W. P. & Ravelo, A. C. Pliocene development of the east-west hydrographic gradient in the equatorial Pacific. *Paleoceanography* **15,** 497–505 (2000).
8. Keller, G. Depth stratification of planktonic foraminifers in the Miocene ocean. *Geol. Soc. Am.* **163,** 177–195 (1985).
9. Kennett, J. P., Keller, G. & Srinivasan, M. S. Miocene planktonic foraminiferal biogeography and paleoceanographic development of the Indo-Pacific region. *Geol. Soc. Am.* **163,** 197–236 (1985).
10. Kamikuri, S., Motoyama, I., Nishi, H. & Iwai, M. Evolution of Eastern Pacific Warm Pool and upwelling processes since the middle Miocene based on analysis of radiolarian assemblages: Response to Indonesian and Central American Seaways. *Palaeogeogr. Palaeoclimatol. Palaeoecol.* **280,** 469–479 (2009).
11. Pagani, M., Liu, Z. H., LaRiviere, J. & Ravelo, A. C. High Earth-system climate sensitivity determined from Pliocene carbon dioxide concentrations. *Nature Geosci.* **3,** 27–30 (2010).
12. Siegenthaler, U. *et al.* Stable carbon cycle-climate relationship during the late Pleistocene. *Science* **310,** 1313–1317 (2005).
13. Lyle, M. *et al.* Pacific Ocean and Cenozoic evolution of climate. *Rev. Geophys.* **46,** RG2002 (2008).
14. DeConto, R. M. *et al.* Thresholds for Cenozoic bipolar glaciation. *Nature* **455,** 652–656 (2008).
15. Foster, G., Lunt, D. & Parrish, R. Mountain uplift and the glaciation of North America — a sensitivity study. *Clim. Past* **6,** 707–717 (2010).
16. Lunt, D., Foster, G., Haywood, A. & Stone, E. Late Pliocene Greenland glaciation controlled by a decline in atmospheric CO_2 levels. *Nature* **454,** 1102–1105 (2008).
17. Knorr, G., Butzin, M., Micheels, A. & Lohmann, G. A warm Miocene climate at low atmospheric CO_2 levels. *Geophys. Res. Lett.* **38,** L20701, http://dx.doi.org/10.1029/2011GL048873 (2011).
18. Müller, P. J., Kirst, G., Ruhland, G., von Storch, I. & Rosell-Melé, A. Calibration of the alkenone paleotemperature index $U^{K'}_{37}$ based on core-tops from the eastern South Atlantic and the global ocean (60°N-60°S). *Geochim. Cosmochim. Acta* **62,** 1757–1772 (1998).
19. Lear, C. H., Rosenthal, Y. & Wright, J. D. The closing of a seaway: ocean water masses and global climate change. *Earth Planet. Sci. Lett.* **210,** 425–436 (2003).
20. Lunt, D. J., Valdes, P. J., Haywood, A. & Rutt, I. C. Closure of the Panama Seaway during the Pliocene: implications for climate and Northern Hemisphere glaciation. *Clim. Dyn.* **30,** 1–18 (2007).
21. Schneider, B. & Schmittner, A. Simulating the impact of the Panamanian seaway closure on ocean circulation, marine productivity and nutrient cycling. *Earth Planet. Sci. Lett.* **246,** 367–380 (2006).
22. Steph, S. *et al.* Early Pliocene increase in thermohaline overturning: a precondition for the development of the modern equatorial Pacific cold tongue. *Paleoceanography* **25,** PA2202, http://dx.doi.org/10.1029/2008PA001645 (2010).
23. Zhang, X. *et al.* Changes in equatorial Pacific thermocline depth in response to Panamanian seaway closure: insights from a multi-model study. *Earth Planet. Sci. Lett.* **317–318,** 76–84 (2012).
24. Boccaletti, G., Pacanowski, R. C., Philander, S. G. H. & Fedorov, A. V. The thermal structure of the upper ocean. *J. Phys. Oceanogr.* **34,** 888–902 (2004).
25. Philander, S. G. & Fedorov, A. V. Role of tropics in changing the response to Milankovich forcing some three million years ago. *Paleoceanography* **18,** 1045, http://dx.doi.org/10.1029/2002PA000837 (2003).
26. Brierley, C. M. & Fedorov, A. V. Relative importance of meridional and zonal sea surface temperature gradients for the onset of the ice ages and Pliocene-Pleistocene climate evolution. *Paleoceanography* **25,** PA2214, http://dx.doi.org/10.1029/2009PA001809 (2010).
27. Fedorov, A., Brierley, C. & Emanuel, K. Tropical cyclones and permanent El Niño in the early Pliocene epoch. *Nature* **463,** 1066–1070 (2010).
28. Fedorov, A. V. *et al.* The Pliocene paradox (mechanisms for a permanent El Niño). *Science* **312,** 1485–1489 (2006).
29. Herbert, T., Peterson, L., Lawrence, K. & Liu, Z. Tropical ocean temperatures over the past 3.5 million years. *Science* **328,** 1530–1534 (2010).
30. Lisiecki, L. E. & Raymo, M. E. A. Pliocene-Pleistocene stack of 57 globally distributed benthic delta $\delta^{18}O$ records. *Paleoceanography* **20,** PA1003, http://dx.doi.org/10.1029/2004PA001071 (2005).
31. Locarnini, R. A., Mishonov, A. V., Antonov, J. I., Boyer, T. P. & Garcia, H. E. in *World Ocean Atlas 2005, NOAA Atlas NESDIS 61* Vol. 1 (ed. Levitus, S.) 182 (US Government Printing Office, 2006).

Supplementary Information is linked to the online version of the paper at www.nature.com/nature.

Acknowledgements We thank the Ravelo laboratory group for discussions. We also thank J. Zachos and P. Koch for comments on the manuscript. L. Lajoie, P. Talmage and T. M. Aung assisted in sample preparation and analysis. D. Andreasen and R. Franks provided analytical support. This research used samples and/or data provided by the Integrated Ocean Drilling Program (IODP). Funding for this research was provided by NSF grant OCE0902047.

Author Contributions J.P.L. and A.C.R. did the primary data analysis and wrote the paper with intellectual feedback from all authors. J.P.L. generated alkenone temperature reconstructions; J.P.L., P.S.D., H.L.F., A.C. and M.W.W. analysed foraminifera $\delta^{18}O$.

Author Information Reprints and permissions information is available at www.nature.com/reprints. The authors declare no competing financial interests. Readers are welcome to comment on the online version of this article at www.nature.com/nature. Correspondence and requests for materials should be addressed to J.P.L. (jlarivie@ucsc.edu).